Product-state control of bi-alkali-metal chemical reactions

Edmund R. Meyer* and John L. Bohn
JILA, NIST, and University of Colorado, Department of Physics, Boulder, Colorado 80309-0440, USA
(Received 11 March 2010; published 14 October 2010)

We consider ultracold, chemically reactive scattering collisions of the diatomic molecules KRb. When two such molecules collide in an ultracold gas, we find that they are energetically forbidden from reacting to form the trimer species K_2Rb or Rb_2K, and hence can only react via the bond-swapping reaction 2 KRb $\rightarrow$ K_2 + Rb_2. Moreover, the tiny energy released in this reaction can in principle be set to zero by applying electric or microwave fields, implying a means of controlling the available reaction channels in a chemical reaction.

DOI: 10.1103/PhysRevA.82.042707 PACS number(s): 34.20.Gj, 34.50.Ez, 34.50.Lf

I. INTRODUCTION

The business of chemical physics is to understand the transformation of reactant molecules into product molecules during a chemical reaction. On the theory side, this is a daunting task, requiring the construction of elaborate multidimensional potential energy surfaces, complemented by classical, semiclassical, or even fully quantum mechanical scattering calculations on these surfaces. For experiments, the goal is to provide as complete a picture as possible via the complete determination of all initial and final states. For initial states, the use of molecular beam techniques provides excellent selection of internal degrees of freedom in the reactant molecules and control over their relative state of motion. For final states, spectroscopic methods can select the relative abundance of the different rotational and vibrational states of the products, providing a wealth of information from which reaction dynamics can be inferred [1].

Recently, the experimental attainment of ultracold molecules has pushed molecular beam technology to its ultimate limit in the following sense: it is now possible to prepare a molecule in a single quantum state in all degrees of freedom, down to the nuclear spin state [2,3]. The molecules are moreover characterized by an extremely narrow range of velocities, as set by gaseous temperatures on the order of μK. This circumstance has enabled orders-of-magnitude control over chemical reaction rates, by simply altering the nuclear spin state of the reactant molecules [4] or by applying an electric field [5]. To probe reactions further, one could imagine transferring the molecules from the prepared ground state to any rovibrational excited state of interest. These advances suggest what is possible when one prepares and manipulates the *initial* states of the chemical reaction.

In this article, we suggest that manipulation of the *final* states may also be possible in certain circumstances. Specifically, exit channels can become either energetically allowed or energetically disallowed as a function of the electric field $\mathcal{E}$. This idea was advanced previously in the context of the H + LiF $\rightarrow$ Li + HF reaction, where it was argued that the exoergicity of the reaction could be shifted via electric fields [6]. Here we point out that, for alkali-metal dimers at ultralow temperature, it is conceivable that a previously exoergic reaction can be completely turned off. This possibility is afforded by the fact that, for alkali dimers, the final states of reaction are not terribly different in energy from the reactants. Specifically, we consider collisions of a pair of KRb molecules, prepared in their vibrational ground state ($v_1 = v_2 = 0$) and particular rotational states n_1 and n_2. These molecules are, in general, subject to two kinds of reactions: the formation of trimers via

$$\mathrm{KRb}(v_1 = 0, n_1) + \mathrm{KRb}(v_2 = 0, n_2) \rightarrow \mathrm{K_2Rb} + \mathrm{Rb} + \Delta E_{\mathrm{trimer}}, \quad (1a)$$

$$\mathrm{KRb}(v_1 = 0, n_1) + \mathrm{KRb}(v_2 = 0, n_2) \rightarrow \mathrm{Rb_2K} + \mathrm{K} + \Delta E_{\mathrm{trimer}}, \quad (1b)$$

and the bond-swapping reaction

$$\mathrm{KRb}(v_1 = 0, n_1) + \mathrm{KRb}(v_2 = 0, n_2) \rightarrow \mathrm{K_2}(v_1' = 0, n_1') + \mathrm{Rb_2}(v_2' = 0, n_2') + \Delta E_{\mathrm{bs}}. \quad (2)$$

We report here two circumstances. (i) The reactions (1) that form trimers are energetically disallowed at ultracold temperatures, as the energy released, $\Delta E_{\mathrm{trimer}}$, is negative and large—a couple thousand wave numbers, 9 orders of magnitude larger than translational kinetic energies in the gas. (ii) By contrast, the bond-rearrangement reactions in (2) produce very small energy differences, since the bonds are all covalent and very similar. In zero field the reaction (2) with $n_1 = n_2 = 0$ is exoergic by $\Delta E_{\mathrm{bs}} = 10.34(8)$ cm^{-1}. Because this released energy is smaller than the vibrational splitting in the reactants (92.40 and 57.78 cm^{-1} in K_2 and Rb_2 respectively), only the $v' = 0$ vibrational levels of K_2 and Rb_2 can be accessed in the reaction [7–9]. This reaction is believed to be barrierless [10] and indeed proceeds rapidly at ultralow temperatures [2].

Moreover, the reactants KRb are polar, whereas the products K_2 and Rb_2 are not; thus the products can only be polarized at comparatively high electric fields. Therefore, the relative energy $\Delta E_{\mathrm{bs}}(\mathcal{E})$ between reactants and products is, in principle, a function of the applied electric field $\mathcal{E}$. Indeed, at fields on the order of several 10^5 V/cm, ΔE_{bs} vanishes and the reaction can be turned off altogether. At fields smaller than this, high-lying rotational final states can be disallowed, thereby changing the possible distribution of product states. For example, removing the exit channels that naturally occur in zero field forces the reaction to proceed in a

*meyere@murphy.colorado.edu

different way. Thereby a different reaction path is presumably probed.

II. NONFORMATION OF TRIMERS

We begin with the first point, that trimer formation (1) is energetically forbidden. As the trimer binding energies have not been measured, we must calculate them from *ab initio* methods. In general, three spin-1/2 alkali atoms can combine to form a trimer with total spin $S = 1/2$ (doublet state) or an excited state with $S = 3/2$ (quartet state). Several calculations of doublet states have been achieved for the homonuclear trimers K_3 [11] and Li_3 [12] and for certain molecular Li_2A systems, where A is an alkali-metal atom [13]. Hauser and co-workers have examined the two doublet surfaces of K_3 at C_{2v} geometries as well as the conical intersection at the equilateral triangle geometry described by the D_{3h} group [11]. Recently, Żuchowski and Hutson have examined the doublet alkali-metal trimers for all species [14].

We employ computational techniques similar to those in Refs. [11,13] to compute doublet ground states within the MOLPRO suite of molecular structure codes [15]. We use the effective core potentials and basis sets of the Stuttgart group for the K (ECP10MDF) and Rb (ECP28MDF) atoms [16]. In addition, to adequately model three-body forces, we augment these basis functions with a diffuse function for each of the s, p, and d orbitals in an even tempered manner as well as add a g function for the K atom.

A. *Ab initio* methods: Dimers

We compare two computational approaches and test by comparing to the known diatomic alkali-metal molecular parameters. For both approaches, we first perform a spin-restricted Hartree-Fock (RHF) calculation on the singlet configuration. The first approach uses the RHF wave function as the foundation for a multiconfiguration self-consistent field (MCSCF) calculation [17,18] with an active space that includes the first excited p orbital of each atom. In addition, we include all states resulting from the ns^0np^1 configurations of each atom. All remaining orbitals are closed, meaning they are energy optimized with the restriction that they remain doubly occupied. After each MCSCF calculation, we perform an internally contracted multireference configuration interaction (MRCI) [19,20] calculation with the same active space as in the MCSCF. The minimum energy is then compared to the dissociation energy evaluated in the separated-atom limit.

In the second approach, we perform a coupled clusters with single, double, and noniterative triples excitations [CCSD(T)] [21] on the $X^1\Sigma$ state at the minimum R_e value obtained from the MCSCF + MRCI calculation. We then performed a geometry optimization followed by a basis set superposition error correction (BSSE) [22] to extract the bond length and dissociation energy of the systems at the RHF-CCSD(T) + BSSE level of theory.

To check the adequacy of these computational methods, we compare their results with the known binding energies of alkali-metal dimers [7–9], as shown in Table I. These results show that approach 1 gets close to the dissociation energy of each diatomic species, but noticeably overestimates the bond length, especially for the heavier alkali-metal systems. By contrast, approach 2 does just as well at predicting dissociation energies, but provides far better bond lengths. With either method, binding energies are clearly reproduced to within a few hundred cm^{-1}. We take this as an empirical measure of the calculations' accuracy.

TABLE I. Molecular properties of the potential energy surfaces for the diatomic molecules K_2, KRb, and Rb_2. Equilibrium bond lengths R_e are in Å and dissociation energies D_e are in cm^{-1} (as measured from the bottom of the well). (1) denotes a calculation performed at the MCSCF + MRCI level while (2) denotes a geometry optimization at the RHF-CCSD(T) level accounting for BSSE.

Molecule	R_e (1)	D_e (1)	R_e (2)	D_e (2)	R_e Expt.	D_e Expt.
K_2	4.16	4293	3.92	4328	3.92	4450.711(5)
KRb	4.33	4039	4.05	4062	4.05	4217.328(5)
Rb_2	4.50	3729	4.18	3741	4.17	3993.53(6)

B. Trimers

Having thus tested the electronic structure methods against known dimer properties, we next apply the same *ab initio* methods to determine the minima of the three-body potential energy surfaces. We first survey surfaces in the T geometry, where the odd-atom-out lies on the perpendicular bisector of the homonuclear pair and the overall electronic wave function has C_{2v} symmetry. This restriction will be relaxed below. Thus we initially restrict ourselves to C_{2v} geometries. As a case study, we will look in detail at the K_2Rb surfaces, but the Rb_2K surfaces are similar.

As a first approach we used the RHF-MCSCF + MRCI method due to its time efficiency. To be consistent with the method employed for dimers, we kept the same active space, which included the first excited p orbital of each atom. We included four states each of $^2B_2$ and $^2A_1$ symmetries, 2 $^2B_1$, 1 $^2A_2$, and 1 $^4B_2$ states in the MCSCF. In each MRCI calculation of the $^2B_2$ and $^2A_1$ surfaces, we included four states as well as the reference symmetries of the other doublets.

The results of the RHF-MCSCF + MRCI calculations are presented in Fig. 1 as contour plots of the potential energy surface (PES) in the two independent bond lengths R_{RbK} and R_{K_2}, for the isosceles triangle geometry. These surfaces show that the $^2B_2$ surface (top panel) possesses the lowest minimum and hence represents the ground state of the trimer in the C_{2v} configuration. This energy minimum occurs near the singlet bond length of the KRb dimer (denoted by a horizontal red arrow near 4 Å), but is intermediate between the singlet and triplet bond lengths of the K_2 dimer [red (near 4.5 Å) and green (near 6 Å) vertical arrows, respectively]. In C_{2v} symmetries, B_2 corresponds to an odd reflection about the bisector of the isosceles triangle. This means that along the K_2 bond the electronic wave function should roughly resemble the K_2 triplet wave function, and so should the bond length. There is then diminished electron density at the center between the two K atoms, and this allows the Rb atom to fill this space, bringing the two K atoms slightly closer together than they would be in the K_2 triplet state alone.

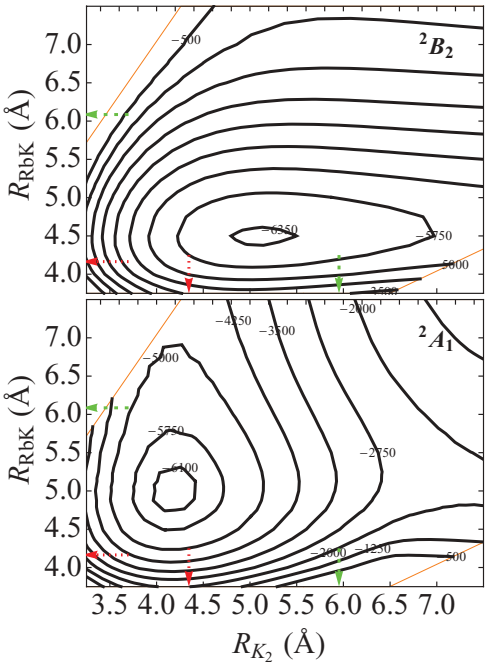

FIG. 1. (Color online) Contour plots for the doublet ground state PESs of K_2Rb versus inter-atomic spacings in an isosceles triangle geometry. The top panel shows the $^2B_2$ surface while the bottom panel shows the $^2A_1$ surface. Contours are labeled in increments of 750 cm^{-1} from −5750 to −500 with an additional contour near the minimum of each surface. The small-dashed red arrows on the vertical (horizontal) axes near 4 Å represent the singlet bond lengths of RbK (K_2). The medium-dashed green arrows on the vertical (horizontal) axes near 6 Årepresent the triplet bond lengths of RbK (K_2).

Similarly, the minimum of the $^2A_1$ surface in the bottom panel of Fig. 1 is located near the K_2 singlet bond length [vertical red (near 4.5 Å) arrow], but in between the singlet and triplet bonds of the KRb system [horizontal red (near 4.0 Å) and green (near 6.0 Å) arrows]. The $^2A_1$ surface requires an even reflection in the electronic wave function across the bisector of the isosceles triangle, therefore preferring a singlet-like bond in R_{K_2}. Therefore, the Rb atom does not quite know which spin to take since it can form a triplet or a singlet with one or the other K atom, but not both. This frustration manifests itself with a bond somewhere intermediate between singlet and triplet bonds in this coordinate.

Knowing that the the RHF-CCSD(T) + BSSE results in the dimer case are markedly better when compared to experimental values, we choose to characterize the minima of the PESs at the RHF-UCCSD(T) + BSSE level of theory. The U in UCCSD(T) refers to the spin-unrestricted formalism due to the open-shell nature of the trimer systems. Starting near the parameters obtained above for the $^2B_2$ surface, we find the optimum geometry by the method of steepest descents. Binding energies are determined at the RHF-UCCSD(T) + BSSE level of theory. The results are presented in Table II for all the alkali-metal trimers containing K and Rb. In the case of K_3, where results have previously been computed, we find excellent agreement with the reported values of the isosceles bond length $r_{iso} = 4.10$ Å and apex angle $\theta_{apex} = 77.13^\circ$ [11].

TABLE II. Molecular properties of the alkali-metal triatomic molecules containing K and Rb. Bond lengths are in Å, angles are in degrees, and dissociation energies, relative to the complete breakup into three free atoms, are in cm^{-1}.

Molecule	Symmetry	r_{hetero}	r_{homo}	θ	D_e
K_3	C_{2v} $^2B_2$	4.10	5.11	90.0	6059
K_2Rb	C_{2v} $^2B_2$	4.26	4.99	90.0	5817
Rb_2K	C_{2v} $^2B_2$	4.26	5.63	90.0	5533
K_2Rb	C_s $^2A'$	4.25	4.06	73.23	5982
Rb_2K	C_s $^2A'$	4.24	4.41	75.00	5611
Rb_3	C_{2v} $^2B_2$	4.40	5.59	90.0	5273

While a minimum of the surface appears to be in the B_2 symmetry of the C_{2v} point group, an examination of the trimers K_2Rb and Rb_2K away from this symmetry is needed in order to determine whether this is a global minimum. Because of the singlet character of the bond in the $^2A_1$ surface across the homonuclear pair, the added electron density may cause an instability in the energy surface. To calculate the bond parameters at bent geometries, we looked at the systems in the C_s point group using the same optimization procedures. In both trimers the bent geometry minimum is found to be the global minimum, making the $^2A_1$ minimum a saddle point. The parameters are given in Table II. r_{hetero} refers to the shorter of the two bonds between heteronuclear pairs when in C_s symmetry. θ is the angle made by A-q-B, where A and B are differing atoms and q is the midpoint between the homonuclear bond. Based on these results, we conclude that the formation of the K_2Rb trimer would require $\Delta E_{trimer} = 2(4217) - 5982 = 2452\ cm^{-1}$ of energy, certainly rendering this reaction impossible at ultracold temperatures. Should the zero-point energy be included in the trimer species, one would find an even larger energy required to form the trimer species. Therefore, we have not calculated the energies of these vibrations.

III. BOND-SWAPPING REACTIONS

Since the trimer formations are forbidden at ultracold temperatures, we now turn to the bond swapping reaction in (2). In Table III, we present the measured dissociation energies and vibrational frequencies for K_2, KRb, and Rb_2. Values are taken from Refs. [7–9]. Here we must use the empirically determined values, as the calculation is accurate to only ∼100 cm^{-1}.

From these values, we find experimentally determined exoergicity in (2) to be $\Delta E_{bs} = 10.35(6)\ cm^{-1}$. That is, the reactants in their ground vibrational and rotational state can only release an energy less than what is available to

TABLE III. Experimentally determined properties for the molecules K_2, KRb, and Rb_2. All energies are in cm^{-1}.

Molecule	D_e	ω_e	D_0
K_2	4450.711(5)	92.40	4404.51
KRb	4217.328(5)	75.85	4179.40
Rb_2	3993.53(6)	57.78	3964.64

produce products in any vibrational state except the ground vibrational state. In the subsections to follow, we present a simple argument for why $\Delta E_{\rm bs} > 0$ in KRb and then suggest how to turn off this chemical reaction with the application of an external electric field.

A. Simple argument

There is a simple argument that relates the energy difference of the reactants (KRb) and products (K_2 and Rb_2) in terms of charge transfer and their respective vibrational constants. Pauling gave a simple picture to relate binding energy of the heteronuclear pair [E(KRb)] to those of the homonuclear dimers [$E(K_2)$ and $E(Rb_2)$], due to charge transfer between the differing atoms [23]. The amount of extra binding energy is

$$c(e_{\rm K} - e_{\rm Rb})^2 = D_e({\rm KRb}) - \tfrac{1}{2}[D_e(K_2) + D_e(Rb_2)], \quad (3)$$

where the constant c depends on the energy units being used and $D_e(AB)$ represents the magnitude of the binding energy of the molecule with respect to the bottom of the well. $e_{\rm K}$ and $e_{\rm Rb}$ are the electronegativities of K and Rb, respectively. They represent the willingness of the atom to accept another electron. As one progresses down the alkali-metal row, the values of e are reduced. In effect, all heteronuclear bonds are strengthened by having charge transfer from one atom to the other; a degree of ionicity is given to the covalent bond. From this simple picture, it appears that two KRb molecules will be more deeply bound than the sum of the binding energies of K_2 and Rb_2. However, this is not the entire picture.

We can enrich this argument by adding the zero-point energy offset due to molecular vibration, that is, work with D_0. We re-express the difference in energy of two KRb molecules and the energy of the K_2 and Rb_2 molecules [$\Delta E_{\rm bs}$ in (2)] in terms of the charge transfer and molecular vibration constants:

$$\begin{aligned}\Delta E_{\rm bs} &= D_0(K_2) + D_0(Rb_2) - 2D_0({\rm KRb}) \\ &= \omega_{\rm AB} - \frac{\omega_{K_2} + \omega_{Rb_2}}{2} - 2c(e_{\rm K} - e_{\rm Rb})^2, \end{aligned} \quad (4)$$

and if this is a positive (negative) quantity then a reaction will (will not) occur. For KRb, the left-hand side of (4) is known empirically. The right-hand side allows us to understand the interplay of charge transfer ($e_{\rm K} - e_{\rm Rb}$) and the zero-point energy offsets, $\omega_{\rm KRb}$, ω_{K_2}, and ω_{Rb_2}. Generally, $\omega \propto 1/\sqrt{\mu}$, where μ is the reduced mass of the system. In the case of KRb, the electronegativities are nearly identical for K and Rb. Therefore, the extra energy associated with transferring charge is negligible. The energy due to vibrations is the dominant energy in Eq. (2). Thus, the mass scalings of the ω values guarantees $\Delta E_{\rm bs} > 0$.

This idea can be extended to LiA molecules, where A is an alkali-metal atom. The offset due to molecular vibration is quite large for Li, and alkali-atoms paired with Li will have vibrational constants closer to that of Li_2 than A_2. Therefore, the term associated with the vibrational constants in (4) will be large and negative, enough that the energy associated with transferring charge is overcome and the system will react to form the homonuclear pairs [14].

B. Electric field suppression of reaction

Because the trimers are energetically forbidden, we now consider the bond-swapping reaction (2) and in particular the variation of $\Delta E_{\rm bs}$ with electric field. To do so, we look at the energy eigenvalues of the reactant and product molecules, as given by the Hamiltonian

$$H = B_e\vec{N}^2 - D\vec{N}^4 - \vec{d}\cdot\vec{\mathcal{E}} - \tfrac{1}{2}\bar{\alpha}\mathcal{E}^2, \quad (5)$$

where B_e is the molecule's rotational constant, D is centrifugal distortion constant, $\vec{d}$ is the body-fixed molecular dipole moment (which is zero for the products), and $\vec{\mathcal{E}}$ is the applied electric field. In addition, both heteronuclear and homonuclear molecules experience a shift due to their electronic polarizability $\bar{\alpha}$. Using the known KRb dipole moment [2] and computed average molecular polarizabilities [24], we can compute the relative energies of the reactants and products.

Because the dipole moment is a function of the internuclear separation R, one is inclined to ask whether the vibrationally excited states of the potential contribute to the shift in energy as a function of the applied electric field. In order to account for the vibrationally excited states, we have used the tabulated dipole moment function of Kotochigova *et al.* [25]. To describe the vibrational wave functions we employ Morse oscillator functions, $\Phi_\nu(R)$, with parameters obtained from the known dissociation energy D_e and equilibrium bond length r_e. We numerically integrate

$$\langle\Phi_\nu(R)|d(R)|\Phi_{\nu'}(R)\rangle = \int \Phi_\nu(R)\, d(R)\Phi_{\nu'}(R)\, dR, \quad (6)$$

and find convergence of the integral using bounds $R_{\rm inner} = 6a_0$ and $R_{\rm outer} = 10a_0$. The functions $\Phi_\nu(R)$ are negligible when less than $R_{\rm inner}$ for all ν and beyond $R_{\rm outer}$ for ν up to 50. Table IV gives the overlap integrals for the first few vibrationally excited states. For $\nu > 4$, the excited wave function has many nodes and thus tends to diminish the product $\Phi_0(R)\Phi_\nu(R)$ regardless of the form of $d(R)$.

The fact that $d(R)$ is nearly constant in the vicinity of $R = r_e$ makes the integrand in Eq. (6) very small except when $\nu = \nu'$. Therefore, we can use second-order perturbation theory to describe how the vibrationally excited states change the rovibrational ($\nu = 0, N = 0$) ground state. In effect, we are defining a polarizability due to vibrational coupling. Recall that the energy levels of a Morse oscillator are given by

$$E(\nu) = \hbar\omega_e(\nu + 1/2)\left(1 - \frac{\hbar\omega_e(\nu + 1/2)}{4|D_e|}\right), \quad (7)$$

TABLE IV. Evaluation of Eq. (6) for the first three excited states. All values are in units of the experimentally determined ground-state dipole moment. Only the upper half is printed for convenience.

	$\nu' = 0$	$\nu' = 1$	$\nu' = 2$	$\nu' = 3$
$\nu = 0$	1	5.1×10^{-3}	-3.2×10^{-4}	1.4×10^{-5}
$\nu = 1$		1	7.1×10^{-3}	-5.5×10^{-4}
$\nu = 2$			1	8.7×10^{-3}
$\nu = 3$				1

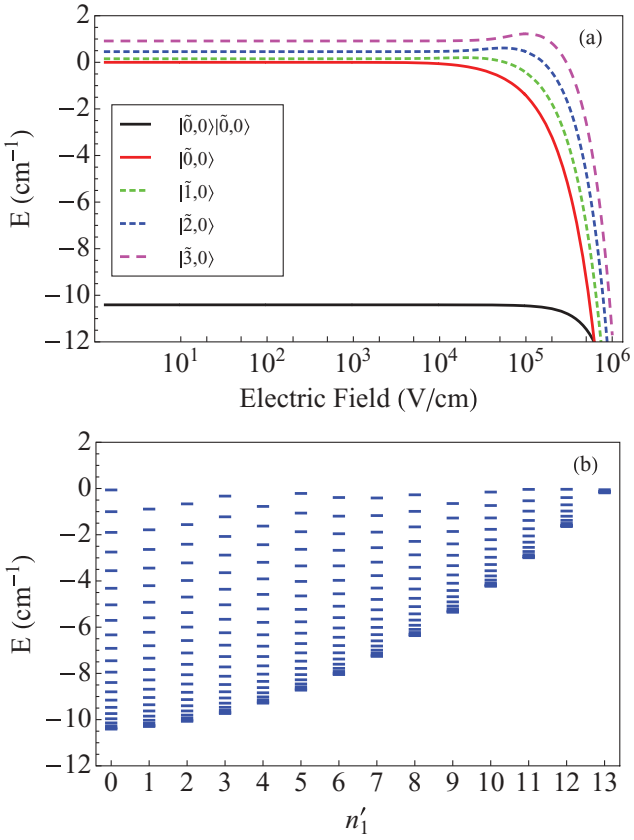

FIG. 2. (Color online) Panel (a) shows the Stark shift for the ground and first few rotationally excited states for a pair of KRb molecules (colored lines) with various dashed spacings. The ground rotational state of KRb is represented by the solid red line (second from the bottom) which starts at 0 cm^{-1} on the vertical axis. The solid black (bottom) line shows the energy of the final states $K_2(v_1' = 0, n_1' = 0) + Rb_2(v_2' = 0, n_2' = 0)$. Panel (b) shows the rotational states energetically allowed at zero electric field. Along the vertical axis is the same scale of energy in cm^{-1}. The horizontal axis is the rotational quantum number n_1' (a dimensionless integer) which describes the rotational state of K_2. Each solid blue line describes a state with the quantum numbers n_1' and n_2' (the rotational number of Rb_2). Each column represents fixed values of n_1' given by the horizontal axis. As you go up a given column of n_1', you get larger values of n_2'.

where D_e is the dissociation energy from the bottom of the well. Therefore, the polarizability of the $v = 0$ state due to vibrationally excited states ($\alpha_{v=0}$) is

$$\alpha_{v=0} = 2 \sum_{v} \frac{|\langle \Phi_0(R)|d(R)|\Phi_v(R)|^2}{E(v) - E(0)}. \tag{8}$$

From this we find a value of $\alpha_{v=0} = 3 \times 10^{-2}\ ea_0^2$. The sum is converged to six decimal places by including terms up to $v = 3$. In comparing this to the value for the average dc polarizability found in [24] of $\bar{\alpha} = 504\ ea_0^2$, we see immediately that the effects of vibration are negligible in comparison.

The physical reason that the vibrationally excited states play little role in the Stark interaction is due to the slow variation of the dipole moment function with internuclear separation over the values of R where the low-lying vibrational wave functions are appreciable. Since the Morse functions are orthogonal, there is little overlap in this region. The high-lying vibrational states do have appreciable amplitude in the region where the dipole moment function is decaying to zero. However, these high-lying states oscillate rapidly in the region where the $v = 0$ wave function is peaked, and the $v = 0$ wave function is zero in the region where the dipole moment function is decaying to zero. Therefore, there is no contribution and we find it justified to ignore the vibrational energy contribution to the polarizability of KRb and just focus on the dc polarizability. Similar arguments hold for why the variation of $\bar{\alpha}$ with internuclear separation is also ignored, as was done in Ref. [24].

In Fig. 2(a), we plot the energy of the ground state (red line, second from the bottom) and several rotationally excited states of KRb + KRb as a function of the electric field. Also shown [black (bottom) line] is the ground-state energy of the products, $K_2(n_1' = 0) + Rb_2(n_2' = 0)$. In zero field, the reactants are their natural 10.35(6) cm^{-1} above the products. As the field increases, the energy of the polar reactant states decreases rapidly, but that of the nonpolar product states decreases far more slowly. Therefore, at a field beyond $\sim 620 \pm 5$ kV/cm, the reactants are actually lower in energy than the products, ΔE_{bs} becomes negative, and the reaction is completely shut off. The bounds on $\mathcal{E}_{bs}$ are obtained from the uncertainty in the exoergicity of the reaction. While a static electric field this large is probably impractical to implement, it may be possible to achieve the required energy shifts in a suitably designed microwave cavity, such as those proposed for trapping polar species [26]. Theory would then naturally have to account for collisions of the field-dressed states [27,28].

As a point of reference, Fig. 2(b) shows the 230 ± 2 energetically allowed states of the products in zero electric field, indexed by their rotational quantum numbers n_1' and n_2'. It is clear that, before the electric field shuts off all reactions completely, it shuts off first higher-n' states and then successively lower-n' states. Recall that the n' distribution of the products is one of the key observables of physical chemistry. The ability to allow only certain values of n' into this distribution will likely provide an even greater wealth of information from such experiments. The detailed effect on chemistry of shutting off successively lower rotational exit channels remains to be explored. It may be hoped, for example, that the new information gleaned would shed additional light on the role of conical intersections in these reactions.

IV. CONCLUSIONS

We have used standard *ab initio* methods to determine the geometry of the heteronuclear trimers K_2Rb and Rb_2K. In addition, we were able to conclude that the trimers cannot form from the collisions of two KRb polar molecules at ultracold temperatures. The only available chemical pathway is to produce K_2 and Rb_2 molecules a mere 10.35(6) cm^{-1} in energy below the reactants. Because the reactants are polar and the products are not, we calculated the field requisite to turn off this chemical reaction and found $\mathcal{E}_{bs} = 620 \pm 5$ kV/cm.

So far we have focused on KRb, since it is the molecule for which ultracold chemistry has recently been demonstrated experimentally. However, there are other reasonable candidates for these experiments, notably RbCs [29], whose reaction is *endothermic* by 28.7 cm^{-1}. Such a reaction would proceed only by placing the reactant RbC molecules into excited states, which could certainly be done. An applied electric field could then still dictate which final channels are available, by moving these rotationally excited states relative to the Rb_2 + Cs_2 products.

ACKNOWLEDGMENTS

The authors acknowledge useful discussions with G. Quéméner and C. H. Greene, as well as funding from the NSF.

[1] R. D. Levine, *Molecular Reaction Dynamics* (Cambridge University Press, Cambridge, UK, 2005).
[2] K.-K. Ni, S. Ospelkaus, M. Miranda, A. Peer, B. Neyenhuis, J. Zirbel, S. Kotochigova, P. Julienne, D. Jin, and J. Ye, Science **322**, 231 (2008).
[3] J. G. Danzl, M. J. Mark, E. Haller, M. Gustavsson, R. Hart, J. Aldegunde, J. M. Hutson, and H.-C. Nägerl, Nature Physics **6**, 265 (2010).
[4] S. Ospelkaus, K.-K. Ni, D. Wang, M. H. G. de Miranda, B. Neyenhuis, G. Quéméner, P. S. Julienne, J. L. Bohn, D. S. Jin, and J. Ye, Science **327**, 853 (2010).
[5] K.-K. Ni, S. Ospelkaus, D. Wang, G. Quéméner, B. Neyenhuis, M. H. G. de Miranda, J. L. Bohn, J. Ye, and D. S. Jin, Nature **464**, 1324 (2010).
[6] T. V. Tscherbul and R. V. Krems, J. Chem. Phys. **129**, 034112 (2008).
[7] C. Amiot, J. Vergés, and C. Fellows, J. Chem. Phys. **103**, 3350 (1995).
[8] C. Amiot and J. Vergés, J. Chem. Phys. **112**, 7068 (2000).
[9] J. Seto, R. le Roy, J. Vergés, and C. Amiot, J. Chem. Phys. **113**, 3067 (2000).
[10] J. N. Byrd, J. A. Montgomery, and R. Côté, Phys. Rev. A **82**, 010502(R) (2010).
[11] A. Hauser, C. Callegari, P. Soldán, and E. Ernst, J. Chem. Phys. **129**, 044307 (2008).
[12] J. N. Byrd, J. A. Montgomery, H. H. Michels, and R. Côté, Int. J. Quantum Chem. **109**, 3112 (2009).
[13] P. Soldán, Phys. Rev. A **77**, 054501 (2008).
[14] P. S. Żuchowski and J. M. Hutson, Phys. Rev. A **81**, 060703(R) (2010).
[15] MOLPRO, version 2010.1, a package of *ab initio* programs, H.-J. Werner, P. J. Knowles, R. Lindh, F. R. Manby, M. Schütz, and others, see [http://www.molpro.net].
[16] I. Lim, P. Schwerdtfeger, B. Metz, and H. Stoll, J. Chem. Phys. **122**, 104103 (2005).
[17] H.-J. Werner and P. J. Knowles, J. Chem. Phys. **82**, 5053 (1985).
[18] P. J. Knowles and H.-J. Werner, Chem. Phys. Lett. **115**, 259 (1985).
[19] H.-J. Werner and P. J. Knowles, J. Chem. Phys. **89**, 5803 (1988).
[20] P. J. Knowles and H.-J. Werner, Chem. Phys. Lett. **145**, 514 (1988).
[21] C. Hampel, K. Peterson, and H.-J. Werner, Chem. Phys. Lett. **190**, 1 (1992).
[22] S. F. Boys and F. Bernardi, Mol. Phys. **19**, 553 (1970).
[23] L. Pauling, *The Nature of the Chemical Bond*, 3rd ed. (Cornell University Press, Ithaca, NY, 1960).
[24] J. Deiglmayr, M. Aymar, R. Wester, and M. Weidemüller, J. Chem. Phys. **129**, 064309 (2008).
[25] S. Kotochigova, P. J. Julienne, and E. Tiesinga, Phys. Rev. A **68**, 022501 (2003).
[26] D. Demille, D. R. Glenn, and J. Petricka, Eur. Phys. J. D **31**, 375 (2004).
[27] A. V. Avdeenkov, New J. Phys. **11**, 055016 (2009).
[28] S. V. Alyabyshev and R. V. Krems, Phys. Rev. A **80**, 033419 (2009).
[29] J. M. Sage, S. Sainis, T. Bergeman, and D. DeMille, Phys. Rev. Lett. **94**, 203001 (2005).